Available online at www.sciencedirect.com

ScienceDirect

Journal of Photochemistry and Photobiology A: Chemistry 197 (2008) 156–169

Journal of Photochemistry and Photobiology A:Chemistry

www.elsevier.com/locate/jphotochem

Synthesis of new perylene imide dyes and their photovoltaic performances in nanocrystalline TiO_2 dye-sensitized solar cells

Jérôme Fortage, Marjorie Séverac, Coralie Houarner-Rassin,
Yann Pellegrin, Errol Blart, Fabrice Odobel*

Laboratoire de Synthèse Organique, UMR 6513 CNRS&FR CNRS 2465, Université de Nantes, Faculté des Sciences et des Techniques de Nantes, BP 92208, 2, rue de la Houssinière, 44322 Nantes Cedex 03, France

Received 29 October 2007; received in revised form 19 December 2007; accepted 26 December 2007
Available online 17 January 2008

Abstract

Eight novel perylene imide derivatives were synthesized to determine the effect of the nature of electron donating substituents on the perylene core (ether or N-amino), the position of the carboxylic acid anchoring group and the presence of a fused benzimidazole moiety on the performances of dye-sensitized solar cells. The photovoltaic efficiency under AM1.5 of these new dyes, although not optimized, ranges from 0.2% until 2.3%. We note the importance of the position-anchoring group, which controls the electron injection efficiency. With respect to the excited-state electron donor strength, four *O*-aryl substituents at the bay position lead to similar effect as two *N*-piperidinyl groups but with a lower propensity to aggregation and give slightly higher photovoltaic performance than the latter. The benzimidazole unit extends the absorbance of the perylene imide to longer wavelengths, but this effect is lower than introducing charge transfer transition with N-amino substituents. Overall, this work shows that perylene imide remains a promising molecular basis for the future design of new fully organic sensitizers for nanostructured TiO_2 solar cells.

Keywords: Dye-sensitized solar cell; Perylene; Organic sensitizer; Photovoltaic; Titanium dioxide

1. Introduction

Photovoltaic is an attractive technology to produce environmental friendly energy from the major renewable source of energy which is the sun. Among the photovoltaic technologies, dye-sensitized solar cells (DSSCs) represent an attractive one because of its potentially low cost. Polypyridine ruthenium complexes are the most studied sensitizers and they give the highest photovoltaic performances [1–3]. Since the year of 2000, increasing research efforts have been devoted to the development of organic sensitizers and reasonable photoconversion efficiencies have been reached with some push–pull type organic chromophores [4–14]. Organic sensitizers are attractive because they usually display higher molar absorptivity and more red-shifted absorption bands than organometallic sensitizers and they could be potentially prepared at a lower cost. On the other hand, they are usually less photochemically stable, a drawback that could limit their use in DSSCs, as already observed with porphyrin sensitizers [15]. Accordingly, we were particularly interested in perylene imide derivatives owing to their unique outstanding chemical, thermal and especially photochemical stabilities [16–18]. They are indeed used as pigments in car paintings [19] and they have been used several times as sensitizers in DSSCs [20–25]. Very recently, a record photoconversion efficiency of 2.6% has been reported by Imahori and co-workers with dipyrrolidinyl perylene bisimide derivatives [26]. Perylene imides are generally poor electron donors since they are rather used as electron acceptor component in photomolecular systems for photoinduced electron transfer [27–29], but this shortcoming may be overcome by chemical modifications [30].

In the present paper, we report the synthesis and the photovoltaic characterizations of a series of new perylene imide sensitizers in view of shedding some light on the molecular features that control the photovoltaic performances of this type of dyes (Fig. 1). In this study, we first investigated the effect of phenoxy (dyes **1**–**6**) or piperidinyl substituents (dyes **7** and **8**) at the bay positions of the perylene core in order to enhance the electron density on the perylene and make it a better electron donor.

---

* Corresponding author. Fax: +33 2 51 12 54 02.
E-mail address: Fabrice.Odobel@univ-nantes.fr (F. Odobel).

1010-6030/$ – see front matter © 2008 Elsevier B.V. All rights reserved.
doi:10.1016/j.jphotochem.2007.12.034

Moreover, these substituents could also limit the aggregation, since these type of dyes are particularly prone to π-stacking [31–34]. Besides, electron rich substituents could induce new charge transfer transitions that are usually beneficial for photovoltaic performances, as already demonstrated with ruthenium polypyridine sensitizers [1–3] or with push–pull metal free dyes [4–14]. The second parameter studied in this work is the position of the anchoring group on the sensitizer that will naturally affect the magnitude of the electronic coupling between the perylene and the TiO_2 conduction band. Finally, the last parameter tested is the influence of the extension of the aromatic system by introducing a benzimidazole unit (dyes **2** and **4**) along the long axis in order to shift the visible absorption bands towards the longer wavelengths [35–37].

2. Experimental

N-(2,5-di-*tert*-butylphenoxy)-perylene-1,6-di(4-*tert*-butylphenoxy)-9-bromo-3,4-dicarboximide (**11**) [38,39], perylene-1,6,9-tri(4-*tert*-butylphenoxy)-3,4-dicarboxylic acid anhydride (**14**) [40], pentadecanamine (**19**) [41] and 1-methyl-3-*n*-propyl imidazolium iodide [42] were prepared according to literature methods. Bis(4,4′-dicarboxylic acid-2,2′-bipyridine) bisthiocyanato ruthenium was purchased from Solaronix.

2.1. *9-(para-Oxybenzoic acid)-O-perylene-N-(2,5-di-tert-butylphenoxy)-1,6-di(4-tert-butylphenoxy)-3, 4-dicarboximide (**1**)*

Compound **11** (46 mg, 52 μmol), 4-hydroxybenzoic acid (72 mg, 0.52 mmol) and K_2CO_3 (216 mg, 1.55 mmol) were dissolved in dry DMF (6 mL). The solution was stirred at 110 °C for 20 h and at 140 °C for 20 h. CH_2Cl_2 was added; the organic phase was washed with water, dried over $MgSO_4$ and concentrated to dryness. The product was purified by column chromatography over silica gel (MeOH/CH_2Cl_2: 0/100 → 10/90), to yield a purple solid (16 mg, 33%). ^{1}H NMR (300 MHz, $CDCl_3$): δ 1.26 (s, 9H, ^{t}Bu), 1.28 (s, 9H, ^{t}Bu), 1.32 (s, 9H, ^{t}Bu), 1.34 (s, 9H, ^{t}Bu), 6.95 (d, 1H, $^3J = 2.10$ Hz, H-aryl-di^{t}Bu), 7.04–7.16 (m, 8H, 4H phenyl + 4H-aryl-^{t}Bu), 7.39–7.43 (m, 5H, 4H-aryl-^{t}Bu + 1H-aryl-di^{t}Bu), 7.54 (d, 1H, $^3J = 8.7$ Hz, H-aryl-di^{t}Bu), 7.62 (t, 1H, $^3J = 8.10$ Hz, H perylene), 8.10 (d, 1H, $^3J = 8.70$ Hz, H perylene), 8.25 (d, 1H, $^3J = 8.10$ Hz, H perylene), 8.30 (s, 1H, H perylene), 8.31 (s, 1H, H perylene), 9.34 (d, 1H, $^3J = 8.70$ Hz, H perylene), 9.45 (d, 1H, $^3J = 8.10$ Hz, H perylene). HR-MS (ESI): *m*/*z*: calcd for $C_{63}H_{59}NO_7$, 964.4189 $[M+Na]^+$; found 964.4182 $[M+Na]^+$.

2.2. *Perylene-1,6,9-tri(4-tert-butylphenoxy)-9-bromo-3,4-(4-carboxylic acid-1,2-benzimidazole) (**2**)*

Compound **14** (31 mg, 40.4 μmol), 3,4-diaminobenzoic acid (13 mg, 80.8 μmol) and zinc acetate (8 mg, 59.4 μmol) were added to 3 mL of dry quinoline. The reaction mixture was heated at 200 °C for 24 h. The quinoline was removed by a distillation, CH_2Cl_2 was added and the organic phase was poured into an aqueous HCl solution (10%). The precipitate was removed by filtration, washed with water, dried under vacuum. The product was purified by column chromatography over silica gel (MeOH/CH_2Cl_2: 0/100 → 2/98), to yield a purple solid (45 mg, 57%). ^{1}H NMR (300 MHz, $CDCl_3$): δ 1.26 (s, 9H, ^{t}Bu), 1.28 (s, 9H, ^{t}Bu), 1.32 (s, 9H, ^{t}Bu), 6.98–7.16 (m, 6H, H phenyl), 7.34–7.44 (m, 6H, H phenyl), 7.58 (m, 1H, H perylene), 7.92 (m, 1H, H-aryl-^{t}Bu), 8.20 (m, 1H, H perylene), 8.25 (m, 2H, H-aryl-^{t}Bu), 8.28 (m, 1H, H perylene), 8.80 (m, 1H, COOH), 8.90 (m, 1H, H perylene), 9.07 (m, 1H, H perylene), 9.13 (m, 1H, H perylene), 9.29 (m, 1H, H perylene). HR-MS (ESI): *m*/*z*: calcd for $C_{59}H_{50}N_2O_6$, 883.3747 $[M+H]^+$; found 883.3817 $[M+H]^+$.

2.3. *N-Octyl-perylene-1,6,7,12-tetra(4-tert-butylphenoxy)-3,4-dicarboximide-9,10-dicarboxylic acid anhydride (**3**) and perylene-1,6,7,12-tetra(4-tert-butylphenoxy)-3,4,9,10-tetracarboxylic acid dianhydride (**17**) [40,43]*

N,*N*′-Dioctyl-perylene-1,6,7,12-tetra(4-*tert*-butylphenoxy)-3,4,9,10-dicarboximide **16** (2 g, 1.66 mmol) was dissolved in a mixture of KOH (266 mg, 4.475 mmol) and *tert*-butanol (67 mL). The solution was stirred at 100 °C for 30 min. Then the crude mixture was cooled to room temperature, an aqueous HCl solution (10%) and water were added. The solution was filtered and the precipitate was washed with water. The solid was dissolved in CH_2Cl_2, the organic phase was dried over $MgSO_4$ and concentrated to dryness. The product was purified by column chromatography over silica gel (petroleum ether/CH_2Cl_2: 6/4) to yield compound **3** (690 mg, 38%) and then compound **17** (647 mg, 40%) as purple solids.

*Compound **3***

^{1}H NMR (300 MHz, $CDCl_3$): δ 0.85 (m, 6H, CH_3), 1.25–1.28 (m, 20H, CH_2), 1.30 (s, 36H, ^{t}Bu), 1.67 (m, 4H, CH_2), 4.06–4.11 (m, 4H, CH_2), 6.80–6.83 (dd, 4H, $^3J = 7.50$ Hz, $^3J = 1.50$ Hz, H-aryl-^{t}Bu), 6.82–6.85 (dd, 4H, $^3J = 7.50$ Hz, $^3J = 1.50$ Hz, H-aryl-^{t}Bu), 7.25 (d, 8H, $^3J = 7.50$ Hz, H-aryl-^{t}Bu), 8.20 (d, 2H, $^3J = 1.50$ Hz, H perylene), 8.22 (d, 2H, $^3J = 1.50$ Hz, H perylene). ^{13}C NMR (75 MHz, $CDCl_3$): δ 14.1, 22.6, 27.1, 28.1, 29.2, 29.3, 31.5, 31.8, 34.4, 40.7, 117.9, 119.3, 119.4, 119.7, 121.5, 122.2, 123.1, 126.7, 126.8, 133.0, 133.3, 147.6, 152.6, 155.8, 156.6, 160.0, 163.4. HR-MS (ESI): *m*/*z*: calcd for $C_{72}H_{73}NO_9$, 1150.5445 $[M+Na+CH_3OH]^+$; found 1150.5466 $[M+Na+CH_3OH]^+$.

*Compound **17***

^{1}H NMR (300 MHz, $CDCl_3$): δ 1.30 (s, 36H, ^{t}Bu), 6.81–6.84 (d, 8H, $^3J = 8.70$ Hz, H-aryl-^{t}Bu), 7.25–7.28 (d, 8H, $^3J = 8.70$ Hz, H-aryl-^{t}Bu), 8.21 (s, 4H, H perylene).

2.4. *N-Octyl-perylene-1,6,7,12-tetra(4-tert-butylphenoxy)-3,4-(4-carboxylic acid-1,2-benzimidazole)-9, 10-dicarboximide (**4**)*

Compound **3** (100 mg, 91 μmol), 3,4-diaminobenzoic acid (28 mg, 0.18 mmol) and zinc acetate (19 mg, 0.14 mmol) were added to 5 mL of dry quinoline. The reaction mixture was stirred

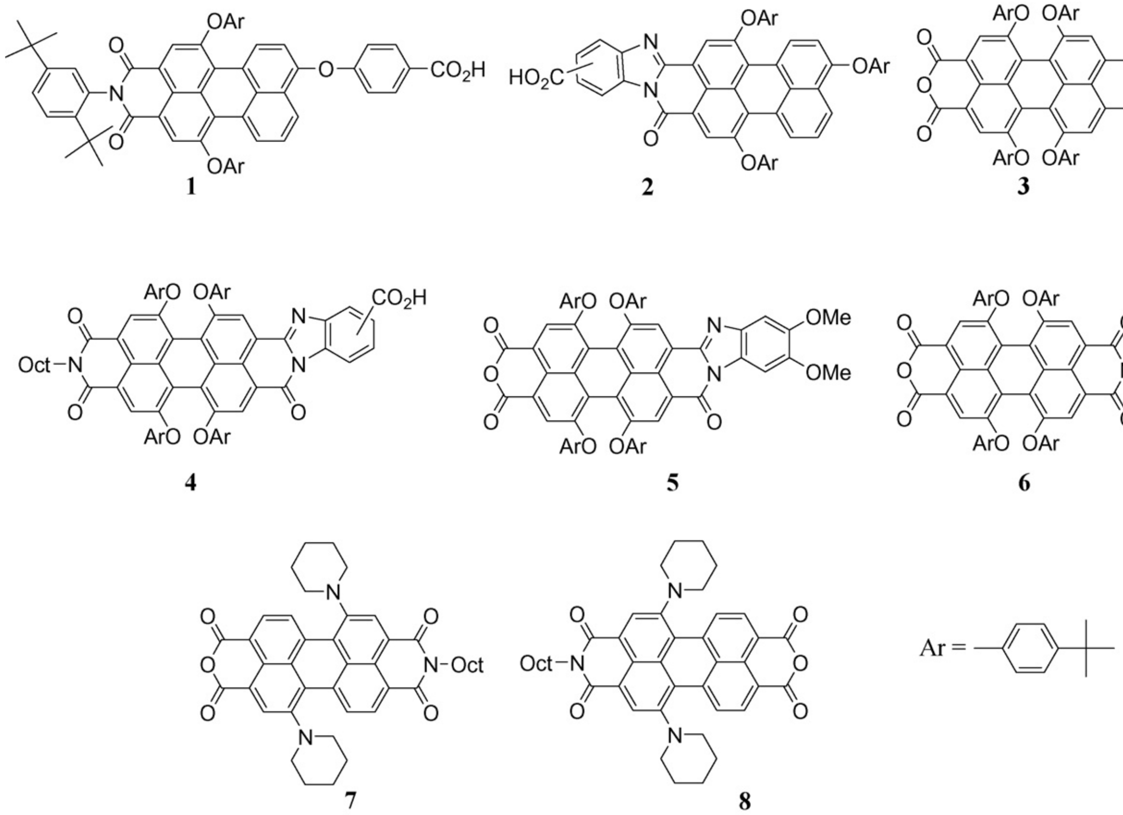

Fig. 1. Structures of the perylene imide sensitizers **1**–**8** prepared and investigated in this study.

at 200 °C for 36 h. The quinoline was removed by distillation, CH_2Cl_2 was added and the organic phase was poured into an aqueous HCl solution (10%). A precipitate appeared, was removed by filtration, washed with water, dried under vacuum. The product was purified by column chromatography over silica gel ($MeOH/CH_2Cl_2$: 0/100 → 2/98) to yield a blue solid (45 mg, 41%). ^1H NMR (300 MHz, $CDCl_3$): δ 0.85 (m, 6H, CH_3), 1.25–1.28 (m, 20H, CH_2), 1.31 (s, 36H, ^{t}Bu), 1.70 (m, 4H, CH_2), 4.10–4.13 (m, 4H, CH_2), 6.79–6.93 (m, 8H, H-aryl-^{t}Bu), 7.26 (m, 8H, H-aryl-^{t}Bu), 7.84–7.86 (m, 1H, H phenyl), 8.20 (m, 1H, H phenyl), 8.21 (s, 2H, H perylene), 8.24 (s, 1H, H phenyl), 8.47 (s, 1H, H perylene), 8.58 (s, 1H, H perylene), 9.23 (s, 1H, COOH). HR-MS (ESI): *m/z*: calcd for $C_{79}H_{77}N_3O_9$, 1212.5738 $[M+H]^+$; found 1212.5728 $[M+H]^+$.

*2.5. Perylene-1,6,7,12-tetra(4-tert-butylphenoxy)-3,4-(4,5-dimethoxy-1,2-benzimidazole)-9,10-dicarboxylic acid anhydride (**5**)*

In a sealed tube, a solution of **17** (100 mg, 0.103 mmol), 1,2-dimethoxy-4,5-diaminobenzene (21 mg, 0.124 mmol) and $ZnCl_2$ (21 mg, 0.155 mmol) in quinoline (5 mL) was introduced. The solution was heated at 180 °C for 6 h. After cooling to room temperature, the solvent was evaporated with a Kugelrohr (under vacuum, 130 °C). CH_2Cl_2 and HCl (6N) were added, the organic layer was extracted with water until pH 7 and dried over $MgSO_4$ before evaporated to dryness. Purification of the residue by column chromatography over silica gel (CH_2Cl_2) gave pure product (32 mg, 28%). ^1H NMR (300 MHz, $CDCl_3$): δ 1.31 (s, 36H, ^{t}Bu), 3.95 (s, 3H, OMe), 4.00 (s, 3H, OMe), 6.86 (m, 9H, 8H-*o*-aryl-^{t}Bu + H-aryl-OMe), 7.27 (m, 8H, H-*m*-aryl-^{t}Bu), 8.02 (d, 1H, $^6J = 6.60$ Hz, H-perylene), 8.21 (m, 2H, H-perylene), 8.43 (t, 2H, $^5J = 8.10$, $^6J = 7.50$ Hz, 1H-perylene + 1H-aryl-OMe). ^{13}C NMR (75 MHz, $CDCl_3$): δ 139.26, 137.06, 134.98, 132.36, 126.77, 126.72, 126.66, 126.58, 122.09, 121.83, 121.68, 120.08, 119.48, 119.39, 119.36, 119.15, 114.60, 114.06, 113.48, 111.62, 34.39, 33.82, 31.92, 31.49, 31.46, 31.41, 29.70, 29.65, 29.62, 29.59, 29.51, 29.35, 29.16, 28.95, 22.95, 14.22. MS (MALDI): *m/z* calcd for $C_{72}H_{64}N_2O_{10}$, 1117.5 $[M+H]^+$; found 1117.8.

*2.6. N-(8-Pentadecanyl)-1,6,7,12-tetra(4-tert-butylphenoxy)perylene-3,4-dicarboximide-9,10-dicarboxylic acid anhydride (**6**)*

A mixture of **20** (0.20 g, 0.14 mmol) and KOH (24 mg, 0.43 mmol) in 3.6 mL of *tert*-butanol was stirred 30 min at 110 °C. The reaction was cooled to room temperature and 4 mL of HCl (10%) then water were added. The mixture was extracted with CH_2Cl_2 and the organic layer was extracted with water until pH 7. The organic layer was dried over $MgSO_4$ and evaporated to dryness. Purification of the solid residue by column chromatography over silica gel (E.P/CH_2Cl_2: 1/1) gave pure purple product (123 mg, 71%). ^1H NMR (300 MHz, $CDCl_3$): δ 0.81 (t, 6H, $^3J = 7.00$ Hz, CH_3), 1.21 (m, 20H, H-aliph), 1.29 (s, 36H, ^{t}Bu), 1.77 (m, 2H, *CH_2*-CH-N), 2.13 (m, 2H, *CH_2*-CH-N), 5.06 (m, 1H, *CH*-N), 6.83 (d, 8H, $^3J = 8.70$ Hz, H-*o*-aryl-^{t}Bu), 7.24 (d, 8H, ^3J = 8.70 Hz, H-*m*-aryl-^{t}Bu), 8.21 (s, 4H, H-perylene). ^{13}C NMR (75 MHz, CDCl$_3$): δ 156.66, 155.76, 155.74, 152.63, 147.7, 147.55, 139.27, 133.13, 126.86, 126.84, 126.81, 126.75, 119.45, 119.28, 119.26, 117.87, 114.05, 54.71, 34.40, 33.82, 32.42, 31.97, 31.93, 31.75, 31.45, 31.41, 30.20, 30.02, 29.47, 29.16, 26.94, 22.88, 22.85, 14.04, 14.00. Emission: 617 and 662 nm. MS (MALDI): *m/z* calcd for $C_{79}H_{87}NO_9$, 1194.6 [M+H]$^+$; found 1194.8.

*2.7. N-Octyl(1,7-dipiperidino)perylene-3,4-dicarboximide-9,10-dicarboxylic acid anhydride (**7**)*

A mixture of *N,N*′-bis(*N*-octyl)(1,7-dipiperidino)perylene-3,4:9,10-bisdicarboximide **28** (0.10 g, 0.13 mmol) and KOH (21 mg, 0.39 mmol) in 3.2 mL of *tert*-butanol was stirred 30 min at 100 °C. The reaction was cooled to room temperature and 3.5 mL of HCl (10%) then water were added. The mixture was extracted with CH_2Cl_2 and the organic layer was extracted with water until pH 7. The organic layer was dried over $MgSO_4$ and evaporated to dryness. Purification of the solid residue by column chromatography over silica gel (CH_2Cl_2) gave pure green product (48.5 mg, 58%). ^{1}H NMR (300 MHz, CDCl$_3$): δ 0.87 (t, 3H, ^3J = 7.50 Hz, CH$_3$), 1.27 (m, 14H, 10H-aliph + H-*p*-piperidine), 1.40 (m, 4H, H-*m*-piperidine), 1.73 (m, 6H, N-CH$_2$-*CH$_2$* + 4H-*m*-piperidine), 2.80 (m, 2H, H-*o*-piperidine), 2.89 (m, 2H, H-*o*-piperidine), 3.37 (m, 4H, H-*o*-piperidine), 4.20 (t, 2H, ^3J = 7.50 Hz, N-*CH$_2$*), 8.25 (m, 3H, H-perylene), 8.37 (s, 1H, H-perylene), 9.23 (d, 1H, ^3J = 8.10 Hz, H-perylene), 9.32 (d, 1H, ^3J = 8.40 Hz, H-perylene). ^{13}C NMR (75 MHz, CDCl$_3$): δ 163.43, 163.25, 160.59, 160.11, 151.23, 150.43, 136.91, 134.61, 130.14, 130.02, 129.95, 127.82, 126.57, 125.44, 124.28, 123.93, 123.88, 123.17, 123.05, 122.48, 121.49, 117.89, 116.05, 52.86, 52.65, 40.62, 31.82, 29.66, 29.63, 29.36, 29.22, 28.15, 27.16, 25.64, 25.55, 25.52, 23.75, 23.72, 22.66, 14.12. MS (ESI): *m/z* calcd for $C_{42}H_{43}N_3O_5$, 670.3 [M+H]$^+$; found 670.4.

*2.8. N-Octyl(1,6-dipiperidino)perylene-3,4-dicarboximide-9,10-dicarboxylic acid anhydride (**8**)*

A mixture of *N,N*′-bis(*N*-octyl)(1,6-dipiperidino)perylene-3,4:9,10-bisdicarboximide **29** (0.07 g, 0.09 mmol) and KOH (15 mg, 0.26 mmol) in 2.2 mL of *tert*-butanol was stirred 30 min at 100 °C. The reaction was cooled to room temperature and 3.5 mL of HCl (10%) then water were added. The mixture was extracted with CH_2Cl_2 and the organic layer was extracted with water until pH 7. The organic layer was dried over $MgSO_4$ and evaporated to dryness. Purification of the solid residue by column chromatography over silica gel (CH_2Cl_2) gave pure blue product (32 mg, 38%). ^{1}H NMR (300 MHz, CDCl$_3$): δ 0.86 (t, 3H, ^3J = 7.50 Hz, CH$_3$), 1.26 (m, 14H, 10H-aliph + H-*p*-piperidine), 1.61 (brs, 4H, H-*m*-piperidine), 1.78 (m, 6H, N-CH$_2$-*CH$_2$* + 4H-*m*-piperidine), 2.86 (m, 4H, H-*o*-piperidine), 3.36 (m, 4H, H-*o*-piperidine), 4.21 (t, 2H, ^3J = 7.50 Hz, N-*CH$_2$*), 8.36 (s, 2H, H-perylene), 8.63 (d, 2H, ^3J = 8.40 Hz, H-perylene), 9.69 (d, 2H, ^3J = 8.40 Hz, H-perylene). ^{13}C NMR (75 MHz, CDCl$_3$): δ 160.47, 153.19, 135.44, 131.93, 130.75, 128.74, 124.45, 124.21, 124.06, 120.87, 118.94, 118.89, 53.06, 52.58, 51.19, 48.95, 48.30, 40.55, 31.92, 31.85, 29.74, 29.69, 29.39, 29.35, 29.24, 29.15, 28.95, 28.20, 27.24, 27.21, 25.77, 23.75, 22.96, 20.36, 14.12. MS (ESI): *m/z* calcd for $C_{42}H_{43}N_3O_5$, 670.3 [M+H]$^+$; found 670.4.

*2.9. N,N′-Octyl-perylene-1,6,7,12-tetra(4-tert-butylphenoxy)-3,4,9,10-dicarboximide (**16**)*

N,N′-Dioctyl-perylene-1,6,7,12-tetrachloro-3,4,9,10-dicarboximide (6 g, 7.97 mmol), K_2CO_3 (11 g, 79.7 mmol) and 4-*tert*-butylphenol (12 g, 79.7 mmol) were dissolved in *N*-methylpyrrolidone (170 mL). The solution was stirred at 130 °C under argon for 20 h. The mixture was chilled to room temperature and an aqueous HCl solution (1N) was added. The solution was filtered and the precipitate was washed with water. The purple solid was dried at 100 °C under vacuum over 2 h. The product was purified by column chromatography over silica gel (petroleum ether/CH_2Cl_2: 6/4 → 0/1) to yield a purple solid (4.85 g, 50%). ^{1}H NMR (300 MHz, CDCl$_3$): δ 0.85 (m, 6H, CH$_3$), 1.25–1.28 (m, 20H, CH$_2$), 1.29 (s, 36H, ^{t}Bu), 1.66 (m, 4H, CH$_2$), 4.07–4.12 (m, 4H, CH$_2$), 6.83 (d, 8H, ^3J = 9.00 Hz, H-aryl-^{t}Bu), 7.23 (d, 8H, ^3J = 9.00 Hz, H-aryl-^{t}Bu), 8.22 (s, 4H, H perylene). ^{13}C NMR (75 MHz, CDCl$_3$): δ 14.1, 22.6, 27.1, 28.1, 29.2, 29.3, 31.5, 31.8, 34.4, 40.7, 119.3, 119.9, 120.5, 122.5, 126.6, 132.9, 147.3, 152.9, 155.9, 163.4. HR-MS (ESI): *m/z*: calcd for $C_{80}H_{90}N_2O_8$, 1206.6697 [M]$^+$; found 1206.6762 [M]$^+$.

*2.10. N,N′-(1-Hexylheptyl)-perylene-1,6,7,12-tetra(4-tert-butylphenoxy)-3,4,9,10-dicarboximide (**20**)*

To a solution of **17** (0.20 g, 0.21 mmol) in DMF (4 mL), 8-pentadecanamine (0.24 g, 1.03 mmol) was added dropwise. The mixture was stirred for 24 h at 150 °C. The reaction was cooled to room temperature and water was added. The mixture was extracted with CH_2Cl_2 and the organic layer was dried over $MgSO_4$ and evaporated to dryness. Purification of the solid residue by column chromatography over silica gel (E.P/CH_2Cl_2: 6/4) gave **20** as pure purple product (225 mg, 78%). ^{1}H NMR (300 MHz, CDCl$_3$): δ 0.81 (t, 12H, ^3J = 7.00 Hz, CH$_3$), 1.20 (m, 40H, H-aliph), 1.29 (s, 36H, ^{t}Bu), 1.77 (m, 4H, *CH$_2$*-CH-N), 2.13 (m, 4H, *CH$_2$*-CH-N), 5.08 (m, 2H, *CH*-N), 6.84 (d, 8H, ^3J = 8.70 Hz, H-*o*-aryl-^{t}Bu), 7.23 (d, 8H, ^3J = 8.70 Hz, H-*m*-aryl-^{t}Bu), 8.21 (d, 4H, ^6J = 8.70 Hz, H-perylene). ^{13}C NMR (75 MHz, CDCl$_3$): δ 155.93, 152.78, 152.76, 147.19, 132.86, 126.63, 119.36, 54.71, 34.35, 32.44, 31.75, 31.46, 29.47, 29.16, 26.94, 22.58, 14.04. MS (MALDI): *m/z* calcd for $C_{94}H_{118}N_2O_8$, 1403.9 [M+H]$^+$; found 1404.1.

*2.11. 1,6- and 1,7-dibromoperylene-3,4:9,10-tetracarboxylic dianhydride (**22** and **23**)*

A mixture of perylene-3,4:9,10-tetracarboxylic dianhydride **21** (2.00 g, 5.1 mmol) and sulphuric acid (16.34 mL, 0.17 mol) was stirred 12 h at room temperature. I_2 (0.047 g, 0.18 mmol) was added and the mixture was heated at 85 °C. Br_2 was then added dropwise and after reflux for 8 h, cool water (5 mL) was added slowly. The precipitate was filtered and washed with water until pH 7. The product was dried under vacuum at 120 °C. A red powder was obtained (2.4 g, 86%). This product was insoluble in common organic solvent.

*2.12. N,N′-Octyl(1,6- or 1,7-dibromo)perylene-3,4:9,10-bisdicarboximide (**25** and **26**) [44–46]*

A solution of previous mixture of perylenes **22** and **23** (0.50 g, 0.91 mmol), octylamine (3.77 mL, 22.7 mmol) and 25 mL of a mixture water/butanol: 1/1 was vigorously stirred at 70 °C for 17 h. The reaction was cooled to room temperature and 6 mL of an aqueous solution of HCl (6N) were added slowly. The mixture was poured in a separatory funnel containing 400 mL of CH_2Cl_2 and washed with water (1 L), and brine (1 L). The organic phase was dried over Na_2SO_4 and evaporated to dryness. Purification of the solid residue by column chromatography over silica gel (CH_2Cl_2) gave the mixture of **25** and **26** (0.36 g, 51%). ^{1}H NMR for the mixture of 1,6- + 1,7-substituted (300 MHz, $CDCl_3$): δ 0.88 (t, 6H, $^3J = 6.90$ Hz, CH_3), 1.28 (m, 20H, H-aliph), 1.73 (quint, 4H, $^3J = 7.20$ Hz, N-$\mathrm{CH_2}$-CH_2), 4.17 (t, 4H, $^3J = 7.50$ Hz, N-CH_2), 8.58 (d, 2H, $^3J = 8.40$ Hz, H-perylene), 8.79 (s, 2H, H-perylene), 9.34 (d, 2H, $^3J = 8.10$ Hz, H-perylene).

*2.13. N,N′-Bis(N-Octyl)(1,6-/1,7-dipiperidino) perylene-3,4:9,10-bisdicarboximide (**28** and **29**)*

To a solution of *N*,*N*′-bis(*N*-Octyl)(1,6-/1,7-dibromo-perylene-3,4:9,10-bisdicarboximide) (0.250 g, 0.33 mmol) in dry THF (20 mL), were added piperidine (19.94 mL, 0.20 mol). The mixture was heated under reflux for 22 h. The reaction was cooled to room temperature and water was added. The aqueous layer was extracted with ethyl acetate and the combined organic layers were washed with water (2 L) until pH 7. The organic layer was dried over $MgSO_4$ and evaporated to dryness. Purification of the solid residue by column chromatography over silica gel (CH_2Cl_2/EP: 7/3) gave **29** (0.08 g, 30%) as a blue product and **28** (0.10 g, 41%) as green product.

*Compound **28***

^{1}H NMR (300 MHz, $CDCl_3$): δ 0.88 (t, 6H, $^3J = 6.90$ Hz, CH_3), 1.28 (m, 24H, 20H-aliph + H-*p*-piperidine), 1.57 (broad s, 4H, H-*m*-piperidine), 1.74 (m, 8H, N-$\mathrm{CH_2}$-CH_2 + H-*m*-piperidine), 2.82 (m, 4H, H-*o*-piperidine), 3.40 (m, 4H, H-*o*-piperidine), 4.21 (t, 4H, $^3J = 7.80$ Hz, N-CH_2), 8.30 (s, 2H, H-perylene), 8.31 (d, 2H, $^3J = 8.10$ Hz, H-perylene), 9.43 (d, 2H, $^3J = 8.10$ Hz, H-perylene). ^{13}C NMR (75 MHz, $CDCl_3$): δ 163.54, 163.48, 150.68, 135.26, 129.74, 127.90, 124.04, 123.57, 123.10, 122.70, 122.32, 120.78, 52.73, 40.63, 31.85, 29.41, 29.24, 28.19, 27.21, 25.71, 23.77, 22.65, 14.09. MS (MALDI): *m/z* calcd for $C_{50}H_{60}N_4O_4$, 780.5 [M$^{\bullet+}$]; found 780.7.

*Compound **29***

^{1}H NMR (300 MHz, $CDCl_3$): δ 0.88 (t, 6H, $^3J = 7.50$ Hz, CH_3), 1.28 (m, 24H, 20H-aliph + H-*p*-piperidine), 1.57 (broad s, 4H, H-*m*-piperidine), 1.77 (m, 8H, N-$\mathrm{CH_2}$-CH_2 + H-*m*-piperidine), 2.87 (m, 4H, H-*o*-piperidine), 3.38 (m, 4H, H-*o*-piperidine), 4.19 (q = 2t, 4H, $^3J = 7.80$ Hz, N-CH_2), 8.39 (s, 2H, H-perylene), 8.62 (d, 2H, $^3J = 8.70$ Hz, H-perylene), 9.72 (d, 2H, $^3J = 8.10$ Hz, H-perylene). ^{13}C NMR (75 MHz, $CDCl_3$): δ 165.26, 163.84, 161.21, 158.36, 156.96, 153.31, 136.10, 135.61, 133.32, 132.83, 130.89, 130.77, 128.82, 127.54, 126.00, 123.79, 123.31, 123.23, 123.15, 122.76, 122.38, 121.74, 120.26, 53.14, 33.81, 31.86, 31.83, 29.69, 29.66, 29.40, 29.34, 29.25, 29.21, 29.15, 28.22, 28.15, 27.27, 27.21, 25.71, 23.77, 22.65, 14.09. MS (MALDI): *m/z* calcd for $C_{50}H_{60}N_4O_4$, 780.5 [M$^{\bullet+}$]; found 780.8.

*2.14. N-Octyl-perylene-1,6,7,12-tetra(4-tert-butylphenoxy)-3,4-dicarboximide-9,10-dicarboxylic acid (**30**)*

N-Octyl-perylene-1,6,7,12-tetra(4-*tert*-butylphenoxy)-3,4-dicarboximide-9,10-dicarboxylic acid anhydride **3** (100 mg, 0.09 mmol) was dissolved in a mixture of KOH (10 mg, 0.18 mmol) and *tert*-butanol (5 mL). The solution was stirred at 100 °C for 3 h. Then the crude mixture was cooled to room temperature, mixed with CH_2Cl_2 and an aqueous NH_4Cl solution was added (pH 7) and the organic phase was extracted. The organic phase was dried over $MgSO_4$ and concentrated to dryness. The crude product was purified by column chromatography over silica gel (CH_2Cl_2 to CH_2Cl_2/MeOH: 95/5) to yield compound **30** (93 mg, 91%) as purple solid. ^{1}H NMR (300 MHz, $CDCl_3$): δ 0.84 (m, 3H, CH_3), 1.25–1.28 (m, 10H, CH_2), 1.30 (s, 36H, ^{t}Bu), 1.65 (m, 2H, CH_2), 4.09 (m, 2H, CH_2), 6.73 (broad signal, 4H, H-aryl-^{t}Bu), 6.83 (m, 4H, H-aryl-^{t}Bu), 7.17 (broad signal, 4H, H-aryl-^{t}Bu), 7.24 (d, 4H, $^3J = 7.50$ Hz, H-aryl-^{t}Bu), 8.15 (broad signal, 2H, H-perylene), 8.22 (d, 2H, $^3J = 4.20$ Hz, H-perylene). ^{13}C NMR (75 MHz, $CDCl_3$): δ 163.60, 163.29, 160.05, 156.58, 155.82, 153.06, 152.58, 147.73, 147.59, 133.26, 133.03, 126.82, 126.75, 123.08, 121.55, 119.67, 119.40, 119.30, 117.95, 40.73, 34.40, 31.77, 31.43, 29.26, 29.17, 28.09, 27.10, 22.59, 14.06. MS (MALDI): *m/z*: calcd for $C_{72}H_{75}NO_{10}$, 1114.5469 [M+H]$^+$; found 1114.5677 [M+H]$^+$.

2.15. Photovoltaic cell preparation and characterization

Conductive glass substrates (F-doped SnO_2 purchased from Solems 5 Ω/sq.) were cleaned with water, rinsed with acetone and ethanol and dried in a nitrogen stream. Then, transparent nanocrystalline TiO_2 films were prepared by doctor blading. The TiO_2 paste was purchased from Solaronix Co. (Nanoxid T). The TiO_2 layer was sintered at 450 °C for 30 min in air after being spread on FTO. After cooling the electrode to room temperature, the electrodes were immersed in a 3×10^{-4} M dye solution overnight at room temperature in a mixture of toluene/ethanol:

1/1 for dyes **1**, **2**, **5** and in dichloromethane for dyes **3**, **4**, **6**, **7** and **8**. The counter electrode was a platinum film sputtered on a FTO glass plate. The surface area of the TiO_2 electrode was 0.5 cm^2. The cells were made by clamping the photoanode with the platinum electrode with the interlayer space filled with an electrolyte. The electrolyte consists in a mixture of 0.6 M 1-methyl-3-*n*-propyl imidazolium iodide, 0.1 M LiI, 0.05 M I_2 in propylene carbonate, according to the conditions described in the manuscript 0.1 M 4-*tert-butyl*-pyridine was added or not (see Table 2). The current–voltage characteristics of the cells were measured by a Keithley model 2601 digital sourcemeter controlled by a computer with the software Labview:2.0 and the photovoltaic cell was illuminated with Oriel lamp calibrated to AM1.5 (air mass) intensity (1000 W m^{-2}).

3. Results and discussion

3.1. Synthesis of the compounds

The synthetic route to prepare the perylene dyes **1–4** is depicted in Scheme 1. The tribromo-perylene monoimide **9** was prepared according to the procedure firstly described by Müllen [36] and refined later by Lindsey [47]. Bis *o*-arylation of the 1,6 positions of the tribromo-perylene **9** was accomplished in 70% yield with *tert*-butyl phenol **10** using the copper-catalysed Ullmann reaction [48]. With the same protocol, tris-*o*-arylation of the perylene **9** was conducted with the same reagents, except a large excess of phenol **10** was used to form perylene **12** in 57% yield. Perylene monoimide **1** was prepared similarly in a 33% yield, by reacting hydroxyl benzoic acid **13** with the perylene monobromide **11**. The synthesis of benzimidazole perylene dye **2** starts with the hydrolysis of the imide group of **12** with potassium hydroxide in *tert*-butyl alcohol form the perylene dicarboxylic anhydride **14** [49]. The benzimidazole group was subsequently introduced by the condensation of the commercially available orthodiaminobenzoic acid **15** with **14** in quinoline with zinc chloride to give **2** with a 57% yield. The latter reaction gave a mixture of two regioisomers that were not separated, but used as such for the rest of the studies.

The preparation of the sensitizers **3–6** starts with the known tetrakis(*tert*-butylphenoxy)perylene bisimide **16** [50] that was initially hydrolyzed with potassium *tert*-butanolate to lead to an equimolar mixture of perylene mono(dicarboxylic anhydride) **3** and the perylene bis(dicarboxylic anhydride) **17** [40,43] that were separated by column chromatography (Scheme 1). The mono(dicarboxylic anhydride) **3** was then reacted with an excess of orthodiamino benzoic acid **15** in refluxing quinoline in presence of zinc chloride to afford perylene **4** as a mixture of two regio-isomers with a 28% yield. These two isomers could not be separated and the mixture of dyes was used as such for the rest of the study. The same conditions were applied to the perylene bis(tetracarboxylic dianhydride) **17** with an excess of 4,5-dimethoxy-1,2-phenylenediamine **18** to furnish the perylene benzimidazole **5** with a 28% yield (Scheme 2). Bisimidation of **17** with pentadecan-8-amine afforded perylene bisimide **20** with 78% yield. One imide group of **20** was then hydrolyzed with potassium *tert*-butanolate to form dye **6** in 71% yield.

The preparation of the dyes **7** and **8** is shown in Scheme 3 and it begins with the bromination of the commercially available perylene-3,4,9,10-tetracarboxylic dianhydride **21** with bromine in refluxing sulphuric acid according to the procedure reported by Müllen and coworkers [45]. This reaction is not selective since a mixture of 1,6-dibromo, 1,7-dibromo and a little amount of 1,6,7-trisbromo perylene were formed [46]. However, this mixture was used in the imidation reaction with octylamine to give the perylenes **25** and **26** that could not be separated at this stage, but in the next step as reported by Franceschin et al. [51]. The next reaction consists in the nucleophilic substitution of the bromo groups by piperidine to give **28** and **29** that were cleanly separated on silica gel column chromatography. Finally, the perylenes **28** and **29** were hydrolyzed with potassium *tert*-butanolate to afford perylene **7** and **8** in 58% and 38% yield, respectively. The differentiation between the structures of **7** and **8** can be made easily from their ^{1}H NMR spectrum, since the structure of **8** is more symmetrical, the protons on the perylene core came as one singlet and two doublets, whereas those of **7** appear as four signals.

3.2. UV–vis absorption and emission properties

The electronic absorption along with emission spectra of the perylene dyes **1–8** and **30** are shown in Fig. 2 and the spectroscopic data are gathered in Table 1.

The perylene dyes **1–6** and **30** display an intense absorption band in the visible spectrum located between 400 and 650 nm corresponding to a $\pi \rightarrow \pi^*$ singlet transition. The three distinct vibronic bands are much better resolved for the dyes having four phenoxy substituents at the bay positions of the perylene core (**3–6** and **30**) than those substituted by three phenoxy groups positioned in a less symmetrical arrangement (**1–2**). The lower degree of symmetry of perylenes **1** and **2** may induce a higher number of vibronic modes which results in a broader absorption band.

The introduction of a benzimidazole group on the perylene core leads to a significant bathochromic shift of absorption maximum and to an enhancement of the molar absorption coefficient (Fig. 2 and Table 1). The extension of the π-conjugation system between the perylene core and the benzimidazole unit, accounts for the narrowing of the HOMO–LUMO gap in the dyes **2**, **4** and **5** [35]. This trend is confirmed by the fluorescence measurements which show that these dyes exhibit the lower singlet excited-state than the corresponding perylene imide (**2** versus **1** and **4** and **5** versus **3**).

The long wavelength absorption band of the push–pull perylenes **7**, **8** and **5** certainly present a charge transfer character corresponding to a shift of the electron density from the electron rich moiety (ether or amino substituents) towards the dicarboxylic anhydride group and it is significantly red-shifted compared to the other dyes. Indeed, it was reported by other groups with other perylene imides substituted with electron rich unit that the most red-shifted band corresponds to a charge transfer transition [52,53].

The spectrum of the perylenes chemisorbed on TiO_2 electrode are shown in Fig. 3 along with those recorded in

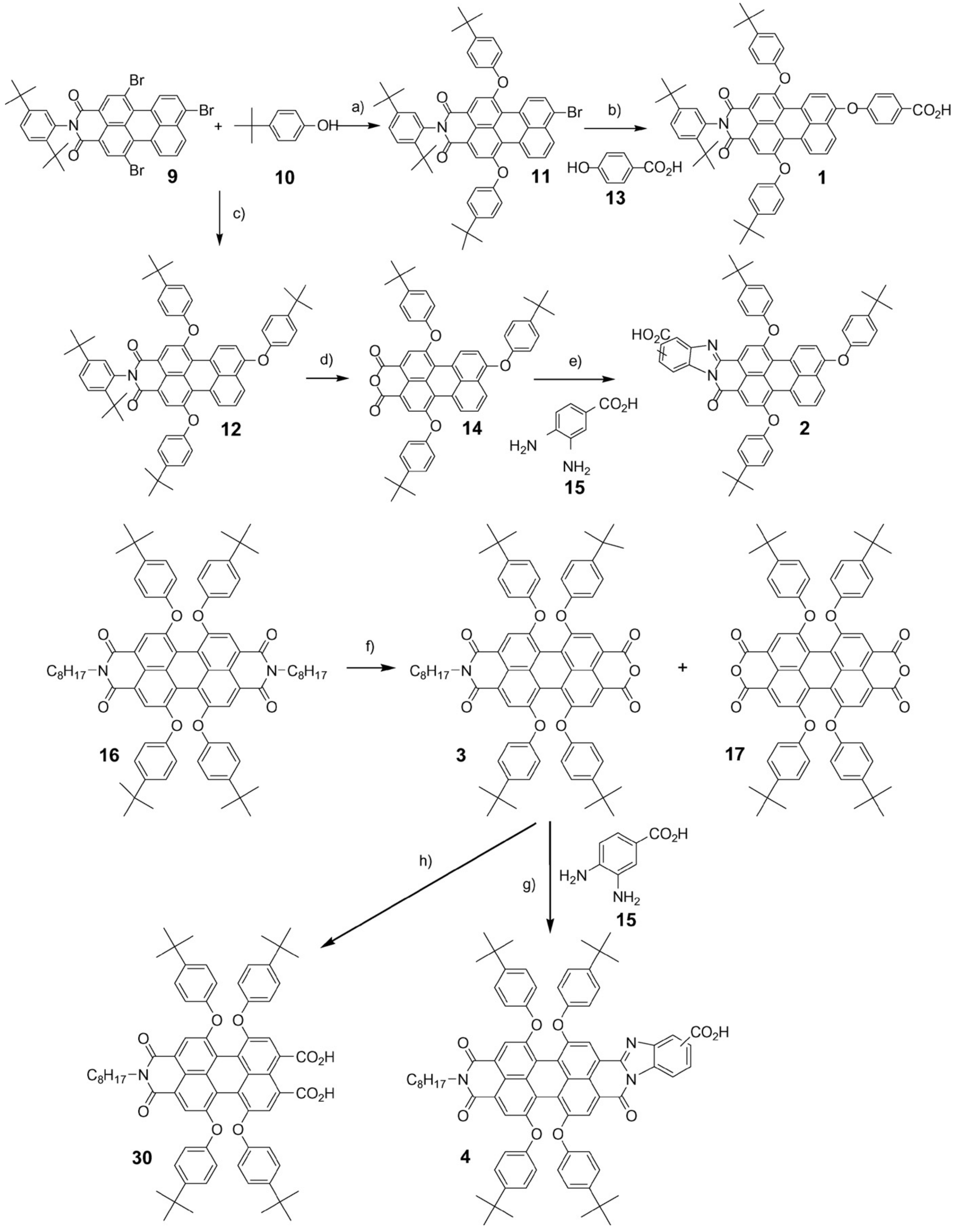

Scheme 1. Synthetic route to the dyes **1**–**4**. Reagents and conditions: (a) Cs_2CO_3, AcOEt, Toluene, CuI, 130 °C, 6 h, 70%; (b) K_2CO_3, DMF, 110 °C, 20 h and 140 °C, 20 h, 33%; (c) DMF, K_2CO_3, 110 °C, 2 h, 57%; (d) KOH, *tert*-butanol, 90 °C, 2 h, 80%; (e) $Zn(OAc)_2$, $2H_2O$, quinoline, 200 °C, 24 h, 57%; (f) KOH, *tert*-butanol, 100 °C, 30 min, 38%; (g) $Zn(OAc)_2$, $2H_2O$, quinoline, 200 °C, 36 h, 41%; (h) KOH, *tert*-butanol, 100 °C, 3 h, 91%.

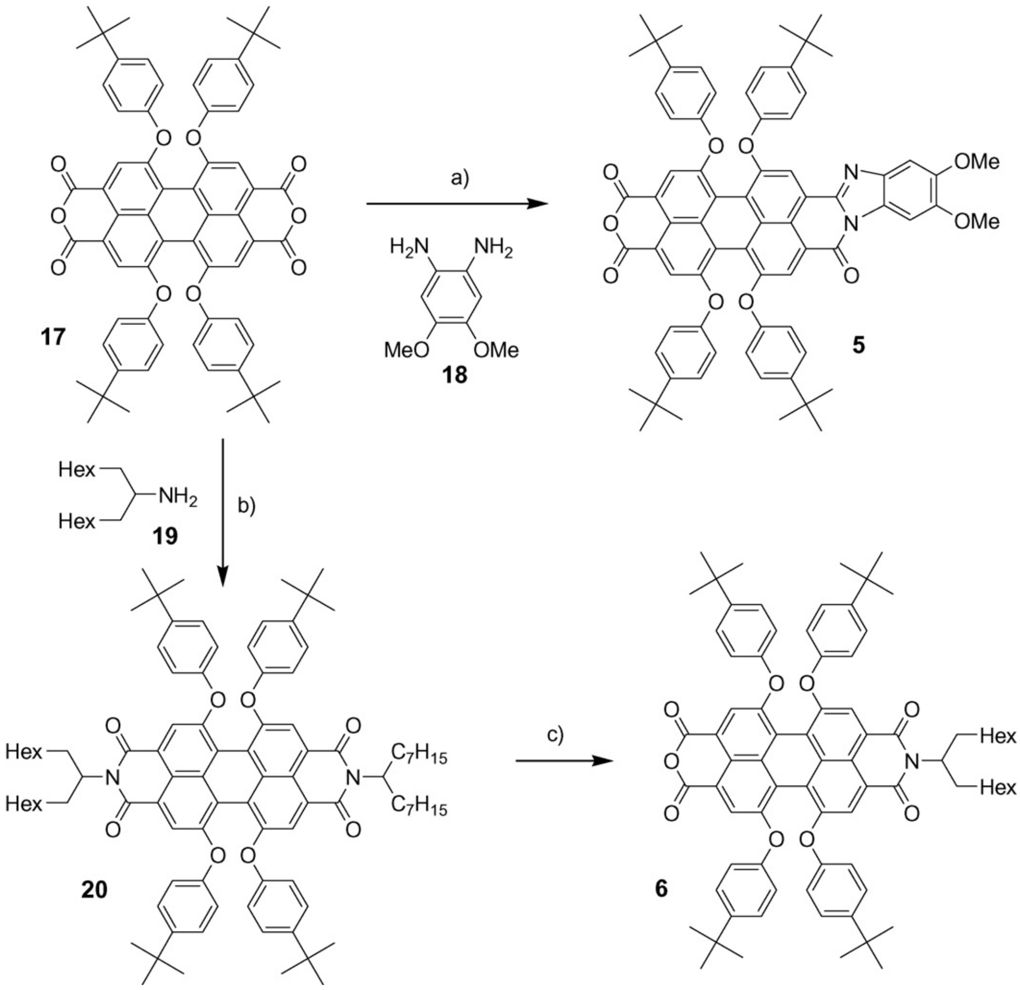

Scheme 2. Synthetic route to the dyes **5** and **6**. Reagents and conditions: (a) $ZnCl_2$, quinoline, 180 °C, 6 h, 28%; (b) DMF, 150 °C, 24 h, 78%; (c) KOH, *tert*-butanol, 110 °C, 30 min, 71%.

Table 1
Absorption, emission and electrochemical data of the perylene imide **1**–**8** and **30** recorded at room temperature in dichloromethane

Dye (D)	λ_{abs} (nm) (ε, M^{-1}/cm^{-1})	λ_{em} (nm) (E_{00}, eV)[a]	E_{Red} (D/D^-) (V)	E_{Ox} (D^+/D) (V)	E^*_{Ox} (V)[c]
1	413 (7200); 487 (21,200); 517 (31,900)	600 (2.24)	−1.03	1.12	−1.12
2	419 (5000); 560 (37,400)	641 (2.06)	−0.98	1.05	−1.01
3	449 (18,600); 538 (27,600); 578 (45,600)	616 (2.06)	−0.64	1.34	−0.72
4	451 (18,300); 563 (45,600); 602 (66,000)	645 (1.99)	−0.67	1.33	−0.66
5	450 (11,300); 626 (27,400)	No detectable emission (∼1.85[b])	−0.62	1.18	∼−0.67
6	451 (11,100); 542 (17,500); 581 (27,800)	616 (2.06)	−0.64	1.35	−0.71
7	416 (10,300); 434 (13,000); 692 (18,000)	780 (1.68)	−0.68	0.86	−0.82
8	648 (11,300)	650 (1.71)	−0.66	0.99	−0.72
30	424 (4400); 504 (6300); 537 (9400)	589 (2.20)	−1.14	1.20	−1.0

All the potentials are referred vs. the saturated calomel electrode (SCE).

[a] Calculated with the wavelength at the intersection of the emission and absorption spectrum with the equation E_{00} (eV) = 1240/λ (nm).

[b] Estimated from the onset of the lowest energy foot of the absorption band.

[c] Calculated from the equation $E^*_{Ox} = E_{Ox} - E_{00}$.

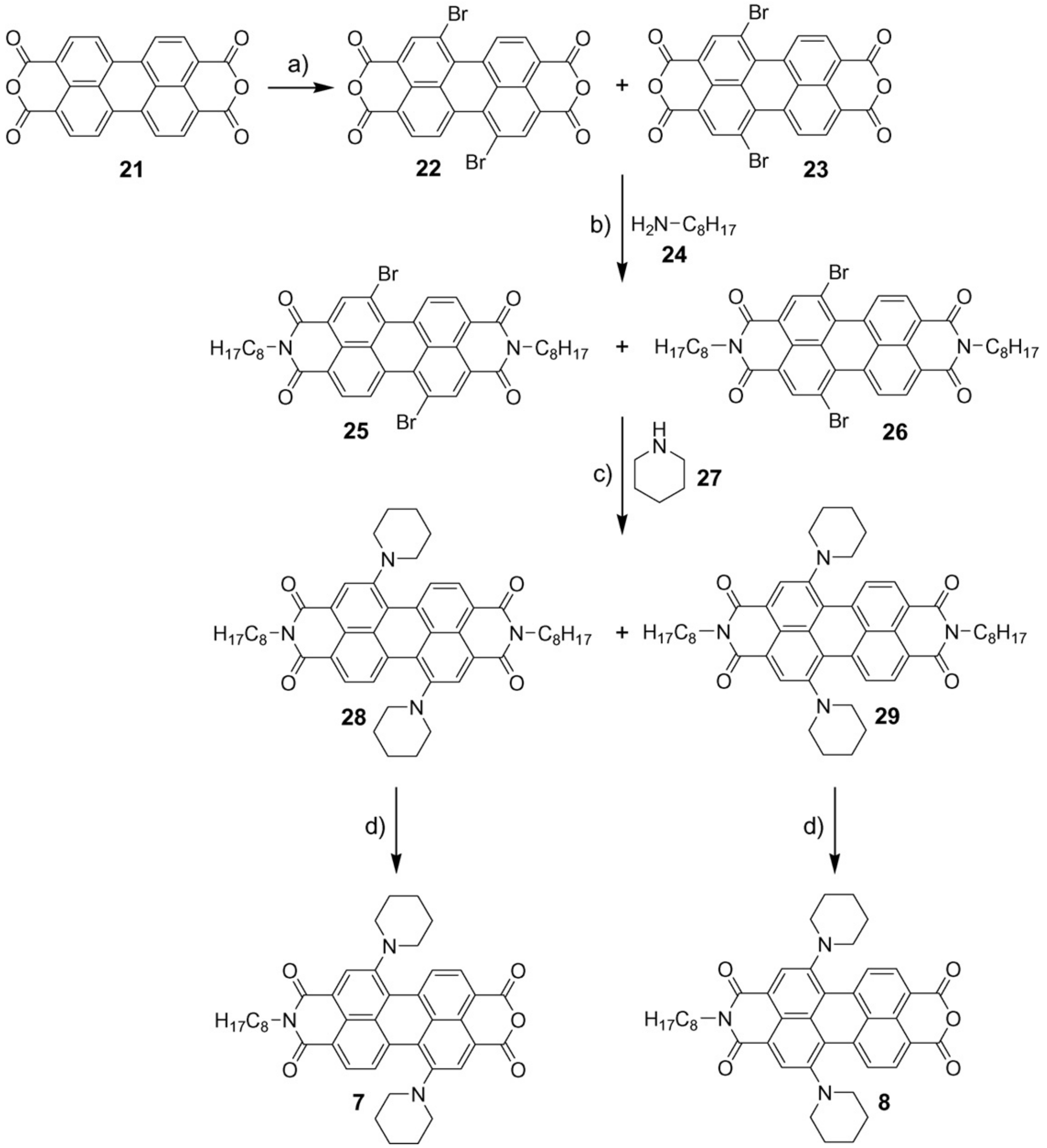

Scheme 3. Synthetic route to the dyes **7** and **8**. Reagents and conditions: (a) sulphuric acid, 12 h at room temperature, I_2, 85 °C, Br_2, reflux, 8 h, 86%; (b) water/butanol: 1/1, 70 °C, 17 h, 51%; (c) THF, reflux, 22 h, 41% (**28**) and 30% (**29**); (d) KOH, *tert*-butanol, 100 °C, 30 min, 58% (**8**) and 38% (**7**).

dichloromethane solution. Interestingly, the spectra of the perylenes containing the dicarboxylic anhydride anchoring group such as in **3**, **5**, **6**, **7** and **8** are significantly blue-shifted upon chemisorption on the TiO_2 electrode compared to that in solution. The chemisorption on TiO_2 most probably arises through the opening of the dicarboxylic anhydride group decreasing thus the π-conjugation of the two carbonyl groups with the perylene owing to a departure from the planarity with the aromatic system. This probably also modifies the degree of the charge transfer character of the transition for the push–pull perylenes. To shed some light on this phenomenon, the dicarboxylic anhydride group of the perylene **3** was hydrolyzed into carboxylic diacid to give perylene **30** (Figs. 2 and 3). The spectrum of this new compound is blue-shifted with respect to that of perylene **3** and it matches quite well that of the dye anchored on TiO_2 (Fig. 3). Furthermore, it is worth noting that the energy of the singlet excited-state has been raised by circa 160 meV upon hydrolysis, supporting the reduced conjugation length in **30** compared to that in **3** (Table 1).

On the other hand, the chemisorption of the dye through the initially available carboxylic acid group, such as in perylenes **1**, **2** or **4**, leads to a broader spectrum than in solution, but with a insignificant modification of the maximum absorption wavelength (Fig. 3). The broadening of the spectrum certainly reflects the aggregation occurring on TiO_2 owing to the formation of π–π perylene stacks, but the energy and the nature of the excited-state are much less altered compared to that of the perylenes containing the dicarboxylic anhydride anchoring group. The apparition of a blue-shifted absorbance for **1** and

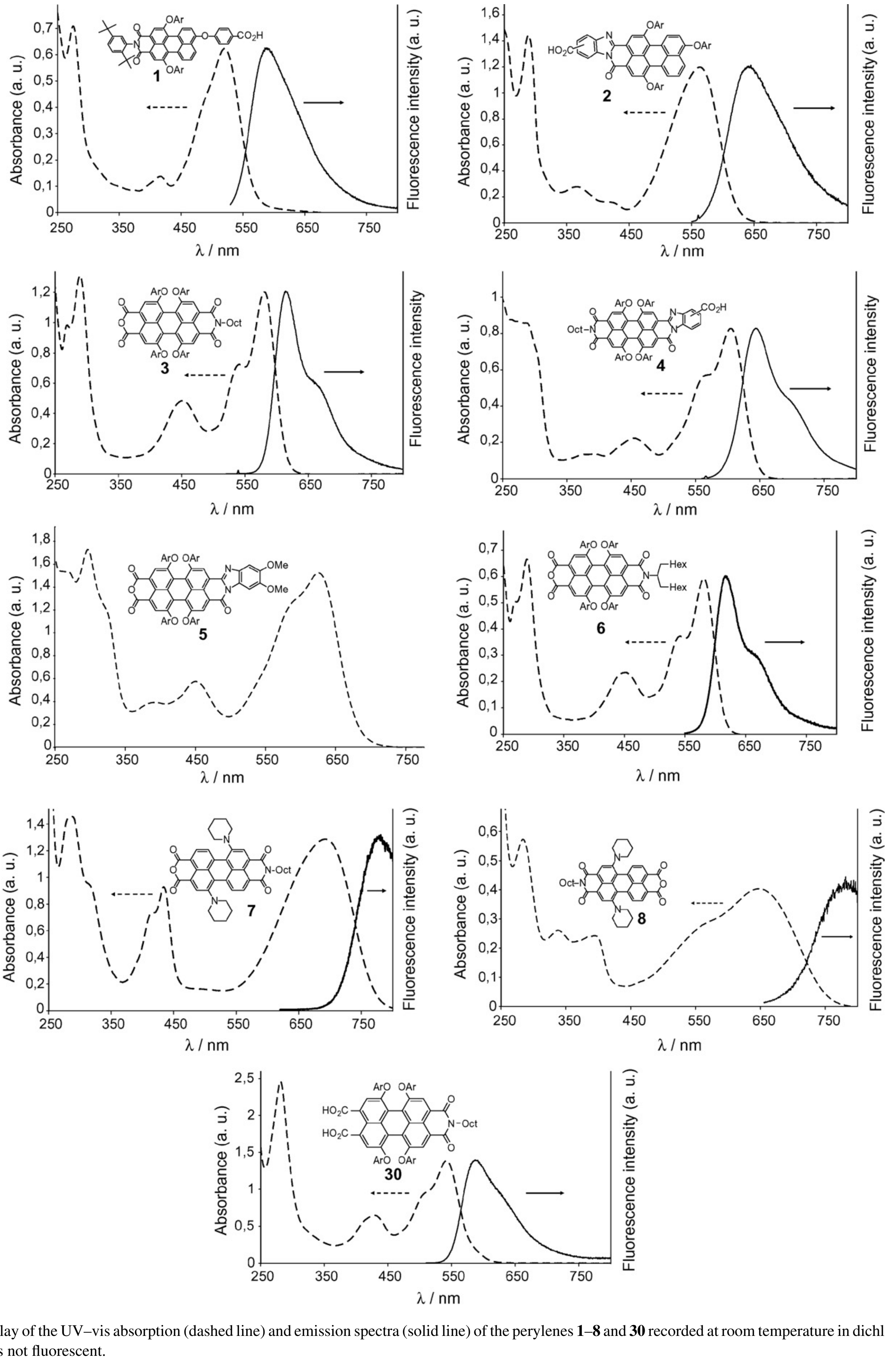

Fig. 2. Overlay of the UV–vis absorption (dashed line) and emission spectra (solid line) of the perylenes **1**–**8** and **30** recorded at room temperature in dichloromethane. Perylene **5** is not fluorescent.

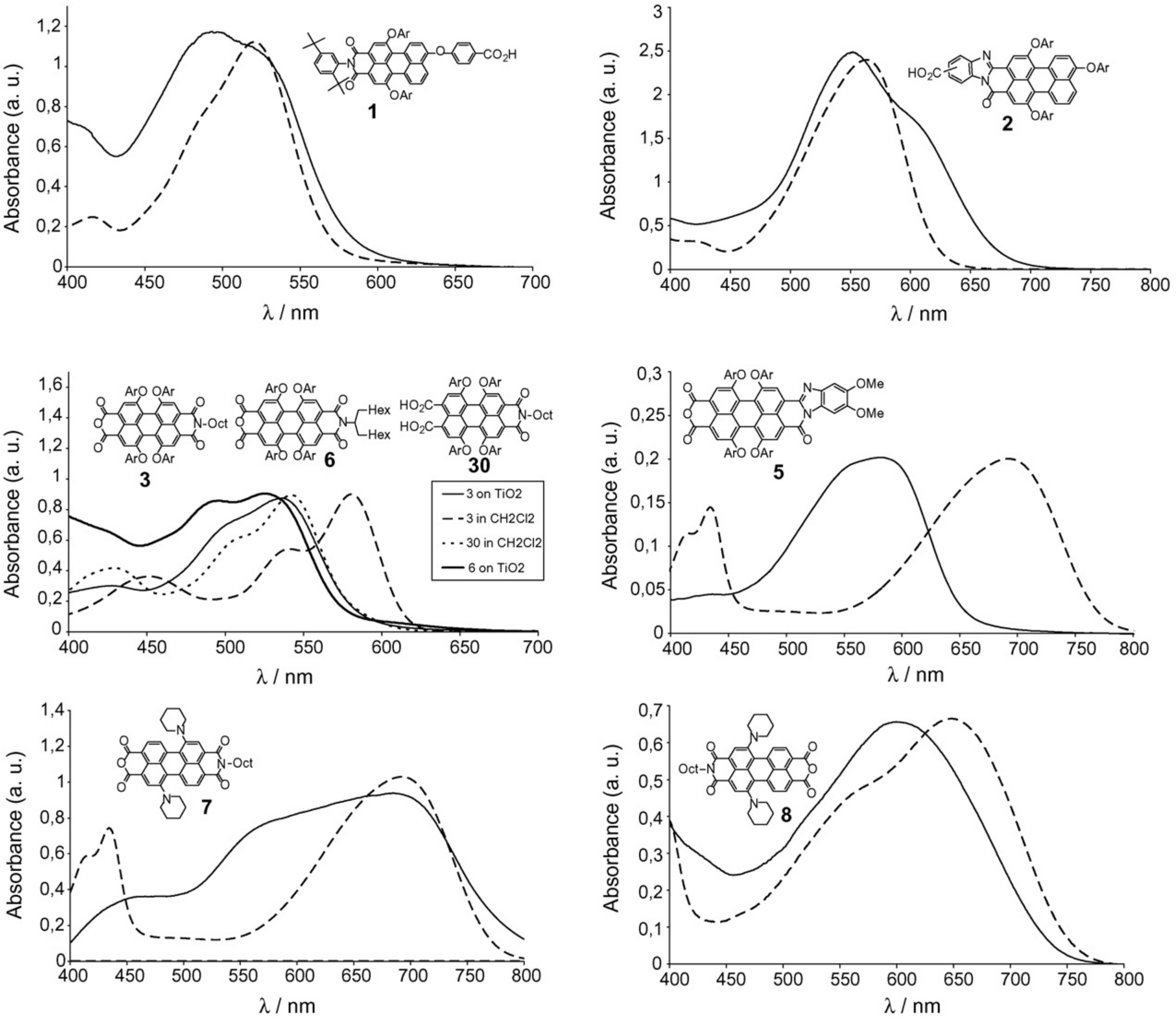

Fig. 3. Overlay of the spectrum of the perylenes **1**, **2**, **3**, **5**, **6**, **7**, **8** and **30** on TiO_2 electrode (solid line) and in dichloromethane solution (dash or dotted line).

a red-shifted band for **2** indicates a different type of molecular organization on TiO_2 [31–33].

3.3. Electrochemical study

Cyclic voltammetry was used to determine the redox potentials of the dyes in order to estimate the driving force of the photoinduced electron injection process. The potentials were recorded in dichloromethane and are referenced versus the saturated calomel electrode (SCE) (Table 1). It is notable that the perylene **30** is easier to oxidize than the parent perylene **3**, indicating that the two carboxylic acid groups in **30** decrease the electron density less than the dicarboxylic anhydride group. As a result, the exact oxidation potentials of the dyes **3**, **5**, **6**, **7** and **8** upon chemisorption on TiO_2 are probably less anodic than those measured in solution.

Knowing that the conduction band potential of TiO_2 is located around −0.7 V versus SCE [1–3], in a first approximation, only the perylene **1**, **2** and **7** exhibit sufficient reducing power to photoinject electrons into the conduction band of TiO_2. However, the chemisorption of the dyes through the hydrolysis of the dicarboxylic anhydride induces both an increase of the energy level of the excited-state and an anodic shift of the oxidation potential of the dyes (Table 1 and Fig. 3). Therefore, if we take into account these two factors, it is very likely that all of these dyes exhibit sufficiently large driving force to photoinject electrons into TiO_2. This is consistent with the relatively high photovoltaic efficiency measured with **5**–**8** and those reported previously by Icli and coworkers with unsubstituted perylene imide dyes, that were even less electron donor due to the absence of electron rich substituents at its bay positions [24].

3.4. Spectrophotoelectrochemical study

The eight perylenes **1**–**8** were used as sensitizer in sandwich type titanium dioxide solar cells and the performances of the cells were investigated while recording the photocurrent photovoltage characteristics (Table 2). For purpose of comparison, the well-known N3 sensitizer (N3 = bis(4,4′-dicarboxylic

Table 2
Results of the photovoltaic performances of the perylenes **1**–**8** recorded under AM1.5

Sensitizer	Electrolyte	V_{OC} (mV)	J_{SC} (mA/cm^2)	ff (%)	η (%)	E^*_{Ox} (V)
1	A	424	2.6	66	0.72	−1.12
	B	440	0.6	83	0.22	
2	A	336	0.9	71	0.21	−1.01
	B	369	0.13	79	0.04	
3	A	443	5.3	63	1.47	−0.72
	B	520	4.1	76	1.64	
4	A	434	1.0	60	0.26	−0.66
	B	461	0.3	81	0.11	
5	A	401	2.9	65	0.76	−0.67
	B	456	2.9	71	0.96	
6	A	494	6.8	62	2.09	−0.71
	B	550	6.2	67	2.29	
7	A	380	5.9	48	1.08	−0.82
	B	450	4.9	64	1.42	
8	A	412	7.6	62	1.96	−0.72
	B	433	3.2	69	0.96	
N3	A	615	14.4	55	4.84	−0.88[a]
	B	663	13.7	62	5.59	

Electrolyte A: 0.6 M 1-methyl-3-*n*-propyl imidazolium iodide, 0.1 M LiI, 0.05 M I_2 in propylene carbonate. Electrolyte B: 0.6 M 1-methyl-3-*n*-propyl imidazolium iodide, 0.1 M LiI, 0.05 M I_2 and 0.1 M 4-*tert*-butyl-pyridine I_2 in propylene carbonate.

[a] Calculated with data from Ref. [44].

acid-2,2′-bipyridine)bisthiocyano ruthenium) was also used as a benchmark reference.

First of all, it is clear that the preparation of the photovoltaic devices is not optimized since the well-known N3 sensitizer gives much lower overall photoconversion efficiency than that reported [2,54]. However, the present conditions permit to compare the dyes between each other and to draw information regarding the factors that affect their relative performances. The overall photovoltaic conversion efficiencies differ significantly with these series of perylene imides and they can be ranked in the following order **6** > **8** > **3** > **7** > **5**∼**1** ≫ **4** ∼ **2**. It is notable that the performance of perylene **6** is similar to the best yield of 2.3% reported by Imahori and coworkers for this class of dyes [26].

The following discussion will be organized according to the different parameters presented in the introduction.

3.4.1. Influence of the binding mode of the perylene on the TiO$_2$

The linking element between the dye and the TiO_2 surface essentially affects the electronic coupling between these two and therefore it controls the rates of the electron injection. The dyes studied here are all anchored to TiO_2 via a carboxylic acid group, but its position on the perylene core varies. It comes either from the opening of a bisanhydric acid group (dyes **3**, **5**–**8**) or it is borne by a benzimidazole (dyes **2** and **4**) or a phenoxy group (dye **1**). The highest photovoltaic performances were systematically obtained with the perylene anchored through the bisanhydric acid binding group (dyes **3**, **5**–**8**), which certainly gives the largest electronic communication with the manifold of TiO_2 conduction band. For dyes **1** and **4**, it is possible to rationalize this result if we observe that the phenoxy and the benzimidazole units are rather electronic rich centres compared to the imide group located at the opposite site of the molecule. As a result, the electronic coupling in the excited-state is certainly reduced, since the electronic density shifts away from the electron rich moieties to reach the most electron withdrawing group, which is unfortunately located far away from the TiO_2 surface (imide group). In the particular case of the perylene **2**, in which no electron deficient centre is present, the low efficiency is certainly caused by the formation of aggregates on TiO_2 which are known to be extremely unfavourable to electron photoinjection [55] These results show the importance of the magnitude of the electronic coupling for this type of sensitizers and demonstrate that bisanhydric acid is the best anchoring group, which is also easily prepared by hydrolysis of the corresponding imide.

3.4.2. Comparison of the O-aryl versus pyperidinyl substituents

O-Aryl and amino-dialkyl substituents were introduced to enrich the electron density of the perylene and to limit its aggregation on TiO_2. As judged from the spectra of these dyes on TiO_2 (Fig. 3), it seems that three *O*-aryl groups do not completely inhibit the formation of aggregates, since broader absorption bands appear upon chemisorption of dyes **1** and **2**. On the other hand, the introduction of four *O*-aryl groups seems to mostly prevent the formation of aggregates since the absorption band of dyes **3**, **6** and **5** on TiO_2 are not particularly broader than in solution, which is also consistent with the fact that these dyes are the best sensitizers of the series. It is notable that the sensitizer **6** is significantly less aggregated than sensitizer **3**, since its visible absorption band is blue-shifted.

N-Piperidinyl substituents tend to limit the aggregation and particularly when these substituents are in *cis* relationship (dye **8**). From the absorption spectra and the values of the oxidation potential, the two *N*-piperidinyl substituents introduce the strongest electron density compared to tetra *O*-aryl substituted perylenes. The dyes **7**–**8** display clear charge transfer transitions that give rise to the most red-shifted absorption bands within these series of compounds (Table 1 and Figs. 2 and 3). Interestingly, the positions of the *N*-piperidinyl substituents have also an impact on the energy of the charge transfer band and consequently on the energy level of the singlet excited-state. The trans *N*-piperidinyl substituents destabilize more the HOMO level than the *cis* isomer, therefore the energy gap with the HOMO orbital is decreased, hence a red-shifted transition and a lower oxidation potential for **7** compared to **8**. In terms of photovoltaic performances, tetra *O*-aryl substituted perylene are a bit superior to *N*-pyperidinyl ones. However, if we compare dyes that have the same alkyl chain at the imide group the differences are not so large (**3** versus **7** and **8**). Indeed, as already noticed by Icli and coworkers [24] and by Imahori and coworkers [26], the substituents on the imide group strongly affect the photovoltaic performances, since the dye **6**, having a branched alkyl chain, exhibits significantly higher photocurrent density than dye **8** with the linear alkyl chain. The origin of this behaviour does not stem from a modification of the electronic properties of these sensitizers since the redox potentials and the excited-state energy levels are identical, which is in agreement with the presence of nodes of the molecular orbitals on the nitrogen of the imide group [16]. The measurements of the current–voltage characteristics in the dark gave almost superimposable curves for **3** and **6** (not shown), indicating a similar blocking effect of the hydrophobic alkyl chain. Interestingly, the spectrum of **3** on TiO_2 is significantly red-shifted compared to that of **6** evidencing higher propensity towards π–π stacking of the former (Fig. 3). This observation is in line with the observation that perylene imides bearing bulky imide groups display reduced aggregation notably with dimethylpentyl substituent and higher solubility than those substituted with linear alkyl chain [56]. The π–π stacked aggregates have usually low emission quantum yield due to self-quenching, explaining thus the lower electron injection efficiency of perylene **3** versus perylene **6**. This is consistent with the idea that losses *via* charge recombination particularly decreases V_{OC}, while J_{SC} is mostly controlled by the electron injection yield although both are correlated to one another. This is exactly what is observed here and in previous works, [22,23] the bulkier imide substituents increase the performances of the cell essentially by an improved J_{SC} (Table 2).

It is notable, that the two isomeric sensitizers **7** and **8**, exhibiting relatively similar electron injection free enthalpy (Table 2), have surprisingly quite different photovoltaic performances. The major difference between these two dyes is certainly the larger transition dipole in the excited-state of **7**, which is experimentally evidenced by a higher absorption coefficient and a longer wavelength maximum absorption and emission bands. In the excited-state of **8**, the electronic density mostly shifts from the amino groups to the nearby bisimide, while in **7** the closer distance of one nitrogen to the anchoring group permit to redistribute more electron density into TiO_2, hence a larger electronic coupling. Consistently, with what was observed with the weakly coupled sensitizers **1**, **2** and **4**, the electron injection yield of perylene **8** drops importantly when the electrolyte contains *tert*-butyl pyridine (Table 2).

3.4.3. Extension of the π-conjugation with benzimidazole unit

The attachment of a benzimidazole moiety on the perylene (dyes **2** versus **1** and dyes **4**–**5** versus **3**) significantly red-shifts the absorption spectrum in agreement with the expected longer delocalization of the π-aromatic system (Table 1 and Fig. 1). However, this effect is not as strong as introducing charge transfer transitions with *N*-piperidinyl substituents.

The benzimidazole moiety being more electron rich than a bisanhydride acid, the former unit should not bear the anchoring group as discussed before. However, if it is placed at the other extremity of the molecule, like in perylene **5**, it can give a real benefit and proved to be relatively efficient, especially if we take into account the weak absorbance of the electrode (Fig. 3). Introduction of stronger electron donating substituents on the benzimidazole, by replacing the methoxy substituents by amino ones for example, could certainly even improve the performances, since perylene **5** displays a quite high oxidation potential and is not a real charge transfer transition.

3.4.4. Influence of tert-butyl-pyridine in the electrolyte

The addition of *tert*-butyl-pyridine in the electrolyte is known to improve the overall photoconversion efficient by increasing the open-circuit voltage owing to upright conduction band bending. The photovoltaic performances of these dyes were investigated with two electrolytes that differ only by the presence or the absence of *tert*-butyl-pyridine. A clear trend appears within these series since the photoconversion efficiencies of **1**, **2**, **4** and **8** drop significantly upon addition of *tert*-butyl-pyridine, while those of perylenes **3**, **5**, **6** and **7** were enhanced, essentially thanks to a larger open circuit voltage (Table 2). Dyes **1**, **2** and **8** exhibit relatively high reducing power in their excited-state (Table 2), therefore the electron injection driving force cannot control entirely the lower performances observed with *tert*-butyl-pyridine. It is rather the weaker electronic coupling that limits the electron injection yield and it becomes critical when the driving force is decreased upon band bending.

In conclusion, we have synthesized and investigated the properties of a series of eight new perylene imide sensitizers that differ with several structural characteristics (binding mode, nature of the substituents on the perylene core, functionalization with a benzimidazole moiety). This study shows that electronic coupling is an important factor that controls the efficiency of the sensitizer and the bisanhydride acid proved to be the optimal anchoring group. The presence of four *O*-aryl groups make the perylene sufficiently electron donating to sensitize TiO_2 efficiently, since relatively high overall photoconversion was obtained with perylene **6**. It is important to underline, the positive effect of bulky branched imide substituents that prevent close packing of the sensitizers on TiO_2 and limit their aggregation. The functionalization of the perylene with a benzimidazole moiety is an effective strategy to extend the absorption spectrum into the red, but it must be preferably placed at the opposite side of the binding group owing to its rather electron rich nature. We believe that these informations constitute useful guidelines for the future molecular design of sensitizers based on perylene imide.

References

[1] A. Hagfeldt, M. Grätzel, Acc. Chem. Res. 33 (2000) 269–277.

[2] B. O'Regan, M. Grätzel, Nature 353 (1991) 737–740.

[3] A. Hagfeldt, M. Grätzel, Chem. Rev. 95 (1995) 49.

[4] N. Koumura, Z.-S. Wang, S. Mori, M. Miyashita, E. Suzuki, K. Hara, J. Am. Chem. Soc. 128 (2006) 14256–14257.

[5] I. Jung, J.K. Lee, K.H. Song, K. Song, S.O. Kang, J. Ko, J. Org. Chem. 72 (2007) 3652–3658.

[6] S. Kim, J.K. Lee, S.O. Kang, J. Ko, J.H. Yum, S. Fantacci, F. De Angelis, D. Di Censo, M.K. Nazeeruddin, M. Grätzel, J. Am. Chem. Soc. 128 (2006) 16701–16707.

[7] T. Horiuchi, H. Miura, K. Sumioka, S. Uchida, J. Am. Chem. Soc. 126 (2004) 12218–12219.

[8] H. Uchida, H. Tanaka, H. Yoshiyama, P.Y. Reddy, S. Nakamura, T. Toru, Synlett (2002) 1649–1652.

[9] S.-L. Li, K.-J. Jiang, K.-F. Shao, L.-M. Yang, Chem. Commun. (2006) 2792–2794.

[10] K. Hara, T. Sato, R. Katoh, A. Furube, Y. Ohga, A. Shinpo, S. Suga, K. Sayama, H. Sugihara, H. Arakawa, J. Phys. Chem. B 107 (2003) 597–606.

[11] K. Hara, M. Kurashige, S. Ito, A. Shinpo, S. Suga, K. Sayama, H. Arakawa, Chem. Commun. (2003) 252–253.

[12] S. Kim, H. Choi, D. Kim, K. Song, S.O. Kang, J. Ko, Tetrahedron 63 (2007) 9206–9212.

[13] M. Liang, W. Xu, F. Cai, P. Chen, B. Peng, J. Chen, Z. Li, J. Phys. Chem. C 111 (2007) 4465–4472.

[14] Z.-S. Wang, F.-Y. Li, C.-H. Huang, L. Wang, M. Wei, L.-P. Jin, N.-Q. Li, J. Phys. Chem. B 104 (2000) 9676–9682.

[15] A. Kay, M. Grätzel, J. Phys. Chem. 97 (1993) 6272–6277.

[16] F. Würthner, Chem. Commun. (2004) 1564.

[17] H. Langhals, Heterocycles 40 (1995) 477–500.

[18] H. Langhals, Helv. Chim. Acta 88 (2005) 1309–1343.

[19] H. Zollinger, Color chemistry, in: Syntheses, Properties, and Applications of Organic Dyes and Pigments, Wiley-VCH, Weinheim,2003.

[20] S. Ferrere, A. Zaban, B.A. Gregg, J. Phys. Chem. B 101 (1997) 4490–4493.

[21] S. Ferrere, B.A. Gregg, J. Phys. Chem. B 105 (2001) 7602–7605.

[22] B.A. Gregg, S. Ferrere, New J. Chem. 26 (2002) 1155–1160.

[23] H. Tian, P.-H. Liu, W. Zhu, E. Gao, D.-J. Wu, S. Cai, J. Mater. Chem. 10 (2000) 2708–2715.

[24] C. Zafer, M. Kus, G. Turkmen, H. Dincalp, S. Demic, B. Kuban, Y. Teoman, S. Icli, Sol. Energ. Mater. Sol. Cell. 91 (2007) 427–431.

[25] H. Langhals, S. Kirner, Eur. J. Org. Chem. (2000) 365–380.

[26] Y. Shibano, T. Umeyama, Y. Matano, H. Imahori, Org. Lett. 9 (2007) 1971–1974.

[27] M.R. Wasielewski, J. Org. Chem. 71 (2006) 5051–5066.

[28] E.H.A. Beckers, S.C.J. Meskers, A.P.H.J. Schenning, Z. Chen, F. Würthner, R.A.J. Janssen, J. Phys. Chem. A 108 (2004) 6933–6937.

[29] T.D.M. Bell, A. Stefan, S. Masuo, T. Vosch, M. Lor, M. Cotlet, J. Hofkens, S. Bernhardt, K. Müllen, M. van der Auweraer, J.W. Verhoeven, F.C. De Schryver, ChemPhysChem 6 (2005) 942–948.

[30] Y. Zhao, M.R. Wasielewski, Tetrahedron Lett. 40 (1999) 7047–7050.

[31] M.J. Ahrens, L.E. Sinks, B. Rybtchinski, W. Liu, B.A. Jones, J.M. Giaimo, A.V. Gusev, A.J. Goshe, D.M. Tiede, M.R. Wasielewski, J. Am. Chem. Soc. 126 (2004) 8284–8294.

[32] W. Wang, L.-S. Li, G. Helms, H.-H. Zhou, A.D.Q. Li, J. Am. Chem. Soc. 125 (2003) 1120–1121.

[33] A.P.H.J. Schenning, J. van Herrikhuyzen, P. Jonkheijm, Z. Chen, F. Würthner, E.W. Meijer, J. Am. Chem. Soc. 124 (2002) 10252–10253.

[34] H. Langhals, R. Ismael, O. Yuruk, Tetrahedron 56 (2000) 5435–5441.

[35] M. Adachi, Y. Nagao, Chem. Mater. 11 (1999) 2107–2114.

[36] H. Quante, Y. Geerts, K. Müllen, Chem. Mater. 9 (1997) 495–500.

[37] I. Lukac, H. Langhals, Chem. Ber. 116 (1983) 3524–3528.

[38] D. Gosztola, M.P. Niemczyk, W. Svec, A.S. Lukas, M.R. Wasielewski, J. Phys. Chem. A 104 (2000) 6545–6551.

[39] D. Gosztola, M.P. Niemczyk, M.R. Wasielewski, J. Am. Chem. Soc. 120 (1998) 5118–5119.

[40] J.-S. Park, C.-W. Lee, M.-S. Gong, Synth. Met. 132 (2003) 177–184.

[41] E.W. Sugandhi, J.O. Falkinham, R.D. Gandour, Bioorg. Med. Chem. 15 (2007) 3842–3853.

[42] V.V. Namboodiri, R.S. Varma, Org. Lett. 4 (2002) 3161–3163.

[43] J. Hua, F. Meng, J. Li, F. Ding, X. Fan, H. Tian, Eur. Polym. J. 42 (2006) 2686–2694.

[44] M.J. Ahrens, M.J. Tauber, M.R. Wasielewski, J. Org. Chem. 71 (2006) 2107–2114.

[45] U. Rohr, C. Kohl, K. Müllen, A. van de Craats, J. Warman, J. Mater. Chem. 11 (2001) 1789–1799.

[46] L. Fan, Y. Xu, H. Tian, Tetrahedron Lett. 46 (2005) 4443–4447.

[47] K.-y. Tomizaki, P. Thamyongkit, R.S. Loewe, J.S. Lindsey, Tetrahedron 59 (2003) 1191–1207.

[48] J. Baffreau, L. Perrin, S. Leroy-Lhez, P. Hudhomme, Tetrahedron Lett. 46 (2005) 4599–4603.

[49] H. Kaiser, J. Lindner, H. Langhals, Chem. Ber. 124 (1991) 529–535.

[50] Y. Li, N. Wang, H. Gan, H. Liu, H. Li, Y. Li, X. He, C. Huang, S. Cui, S. Wang, D. Zhu, J. Org. Chem. 70 (2005) 9686–9692.

[51] M. Franceschin, A. Alvino, G. Ortaggi, A. Bianco, Tetrahedron Lett. 45 (2004) 9015–9020.

[52] J. Ahrens M, J. Tauber Michael, R. Wasielewski M, J. Org. Chem. 71 (2006) 2107–2114.

[53] C.-C. Chao, M.-k. Leung, Y.O. Su, K.-Y. Chiu, T.-H. Lin, S.-J. Shieh, S.-C. Lin, J. Org. Chem. 70 (2005) 4323–4331.

[54] M.K. Nazeeruddin, A. Kay, I. Rodicio, R. Humphry-Baker, E. Mueller, P. Liska, N. Vlachopoulos, M. Grätzel, J. Am. Chem. Soc. 115 (1993) 6382–6390.

[55] S. Tatay, S.A. Haque, B. O'Regan, J.R. Durrant, W.J.H. Verhees, J.M. Kroon, A. Vidal-Ferran, P. Gavina, E. Palomares, J. Mater. Chem. 17 (2007) 3037–3044.

[56] H. Langhals, O. Krotz, K. Polborn, P. Mayer, Angew. Chem. Int. Ed. 44 (2005) 2427–2428.